CRDF GRANT ASSISTANCE PROGRAM

Grant # RUE2-1615-MO-06

A STUDY OF PRE-STRESS EFFECT ON DYNAMIC FAILURE OF TRANSPARENT BRITTLE MATERIALS

Final Technical Report

by

G.I. Kanel, S.V. Razorenov, A.S. Savinykh,
G.S. Bezruchko, G.V. Garkushin, G.E. Ivanchikhina

Institute for High Energy Densities of Russian Academy of Sciences,
Izorskaya 13/19, Moscow, 125412 Russia

(March 2007)

LIST OF ALL PARTICIPATING SCIENTIFIC PERSONNEL

1. Kanel G.I. – Principal investigator
2. Razorenov S.V.
3. Savinykh A.S.
4. Bezruchko G.S.
5. Garkushin G.V.
6. Ivanchikhina G.E.

Contents

A STUDY OF PRE-STRESS EFFECT ON DYNAMIC FAILURE OF TRANSPARENT BRITTLE MATERIALS

G.I. Kanel, S.V. Razorenov, A.S. Savinykh,
G.S. Bezruchko, G.V. Garkushin, G.E. Ivanchikhina

Institute for High Energy Densities of Russian Academy of Sciences

Abstract

The report presents results of studying the pre-stress effect on dynamic failure of K8 crown glass, K14 crown glass, fused quartz and sapphire crystals. A technology of radial pre-compression of glass samples has been worked out. Controlled confinement pressure on the specimen in a range of 150 MPa to 550 MPa was provided by installing a shrink-fit metal sleeve on the lateral surface of the glass specimen disk. Results of measurements of the particle velocity histories of sock-loaded free and pre-stressed glasses confirm our expectation of influence of transversal stress upon the failure wave propagation and the failure threshold: for all pre-stressed glasses we observed earlier break of the failure wave propagation at unloading from shock-compressed state. However, sensitivity of the failure threshold to the confinement stress value is not as high as it could be expected. Large heterogeneity of inelastic deformation and scatter in the Hugoniot elastic limit of sapphire have not allowed us to determine an influence of pre-stressing on the HEL value of this material. However, the experiments unambiguously demonstrate growth of viscosity of inelastic compression of the sapphire as a result of pre-stressing.

1. Introduction

Planar impact experiment is a widely used way to obtain quantitative information about the resistance of materials to inelastic deformation at high-rate compression and about the material response in subsequent unloading [1]. The loading conditions of planar impact tests are of the uniaxial strain state that simplifies interpretation of the shock-wave tests. On the other hand, the uniaxial strain condition does not allow variation of a relationship between longitudinal and transversal stresses. Meanwhile it is known the compressive response of brittle materials is very sensitive to the stress state. At low-stress confinement (or at the absence of confining stress) the offset of the compressive fracture by axial cracking takes place immediately on reaching some threshold stress (failure threshold) and results in the immediate drop of the material load-carrying capacity. The increase of the confining stress suppresses the axial cracking shifting the failure threshold towards the higher stress values. Further increase of the confining stress may result in a transition from brittle to ductile mode of inelastic deformation which does not imply immediate lost of strength.

Several recent research works are known which are devoted to studying the pre-stress effects on dynamic failure of brittle materials. Chen and Ravichandran [2, 3] in their experiments with split Hopkinson pressure bar techniques provided controlled confinement pressure on the specimen by installing a shrink-fit metal sleeve on the lateral surface of the cylindrical ceramic specimen. In this way they have measured the compressive failure threshold as a function of lateral stress for aluminum nitride ceramic. Zaretsky et al. [4, 5] used this technique of varying the transversal stress in the planar impact experiment. Utilizing an essential difference between the dependencies of brittle failure threshold and ductile yield strength on the lateral pressure, they have found that the response of the alumina ceramic to shock-wave compression is ductile whereas the response of boron carbide ceramic is certainly brittle. Han and Sun [6] studied response of layered plates consisting of glass and aluminum layers to static indentation and dynamic impact load. Significant thermal residual stresses were induced in the layered plate bonded at an elevated temperature. The results indicate that thermal residual stresses can delay the onset of contact failure in the glass. However, the benefit of thermal residual stresses in protecting the structure from fracture failure seems to diminish once the projectile achieves substantial penetration into the layered target. Holmquist and Johnson [7] performed computer modeling of pre-stressed ceramic and its effect on ballistic performance. They have found that pre-stressing the ceramic enhanced the ballistic performance, although the effect of the different pre-stress conditions on the ballistic response was not always obvious. Millett and Bourne [8] studied propagation of the failure wave in shocked soda-lime glass as a function of internal stresses. This has been varied by either examining the material in the as-received or a heat-treated state; no values and signs of internal stresses were determined. Results show that while the stressed states of shock-compressed glass do not seem to be significantly effected, failure wave velocity is reduced by an annealing treatment.

In this project we performed quantitative study of the pre-stress effect on the response of homogeneous brittle materials to shock-wave compression. With this goal, experiments with three glasses and sapphire crystals have been carried out.

Silicate glasses demonstrate high Hugoniot elastic limit (HEL) and the spall strength (dynamic tensile strength which does not include the surface effects) more than 6 GPa at peak stresses below the Hugoniot elastic limit as well as above it [1,9]. It is well known, however, the static tensile strength of glasses is very low (around 0.1 GPa). The reason for such a large discrepancy is that the fracture nucleation sites in homogeneous glass are concentrated on the surface. These incipient microcracks are activated and determine the strength magnitude in the static measurements. The impact loading of glasses can be accompanied by an appearance of a failure wave. The failure wave is a network of cracks that are nucleated on the surface and propagate into the stressed body [1, 10].

Among hard transparent materials, sapphire has highest elastic limit and highest spall strength at shock loading below the HEL, but its tensile strength drops to zero when the HEL is exceeded. It is not clear yet whether the vanishing of spall strength is a result of compressive fracture or it is a consequence of violation of the matter homogeneity in course of plastic deformation. One may hope that pre-stressing can suppress compressive fracture in this case also.

Cracks may relatively easy propagate through the crystals in some certain crystallographic directions. Both glasses and single crystals are initially homogeneous in bulk so the fracture nucleation sites may be formed in course of plastic deformation only. In this sense the difference between single crystals and glasses is in that hard crystals have only a limited number of crystal planes and directions in which the usual mechanisms of ductility may work, whereas the ductility of amorphous glasses is completely isotropic. The impossibility of plastic shear along arbitrary directions in crystals results in stress concentration at points of intersections of slip bands or twins that, in turn, may result in cracking at compression or unloading. Ductility of glasses is caused by a loose microstructure with a large amount of molecular-size voids. It is known that glasses show gradual structural changes resulting in increased density. It is supposed that the irreversible densification and compaction in the silicate structure are responsible for the isotropic plastic flow properties of glasses under high pressure.

2. Materials

Tested materials were K8 crown glass, K14 crown glass, fused quartz, and sapphire crystals of c-orientation. Main mechanical properties of these materials are listed in Table 1. In main experimental series the glass samples were 22 mm in diameter and 3.5 mm in thickness. Since it was found earlier that the shock-wave behavior of lapped glass is much more reproducible than that of as-received plates, the glass plates were lapped with SiC powder of 40 μm grain size. Sapphire samples were 22 mm in diameter and 5 mm in thickness. Their planes were parallel to the basal or *c*-plane {0001} of the crystal lattice.

In order to characterize failure properties of the glasses, Figures 1 and 2 present the experimental results [11, 12] with single thick plates and assembled thin plates of fused quartz and K8 crown glass, which demonstrate the appearance of the failure waves in these materials. In the glass plate assemblies, the stress magnitude at elastic wave front should approach the failure threshold which is estimated to be between 7 GPa and 7.7 GPa for fused quartz and 5.3 GPa for K8 crown glass.

Table 1.

Material	ρ, g/cm^3	c_l, km/s	Poisson's ratio, ν	HEL, GPa
Fused quartz	2.205	5.95	0.18	8.7 [13]
K8 crown glass	2.51	6.00	0.209	8 ± 1 [12]
K14 crown glass	2.53	5.90	0.203	
Sapphire	2.45	11.19		12–21 [14]

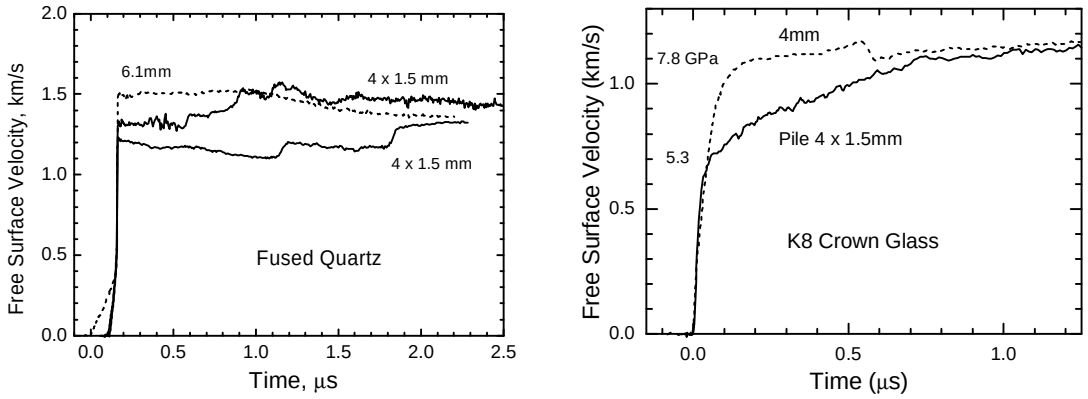

Fig. 1. Experimental results [11, 12] with single thick plate and assembled thin plates of fused quartz impacted by aluminum flyer plates of 4 mm in thickness at 1.5 km/s and 7 mm at 1.17 km/s, respectively.

Fig. 2. Free surface velocity histories of single thick plate and assembled thin plates of K8 crown glass impacted by an aluminum flyer plate of 7 mm in thickness at 1.15 km/s velocity [11, 12].

Figure 3 presents results of analogous experiment with K14 crown glass made in framework of this project. The failure threshold of K14 crown glass is estimated from Fig 3 to be 6.2 GPa that is between K8 glass and fused quartz. K8 and K14 glasses demonstrate slightly different ramping of elastic compression waves that is seen in Fig. 4. We consider the failure threshold values obtained from experiments with glass piles as upper estimations. In reality these values can be lower and are not reached with limited amount of plates in the piles.

The wave profile for single plate of K14 crown glass in Fig. 3 contains small recompression step which is due to the wave reflection from a failed layer inside the sample. Such recompression pulses are usually considered as a signature of the failure wave phenomenon. Consideration of the time distance diagram shows that the failure wave speed may be determined by means of measurement of the time interval t_r between arrivals of the initial compression wave and the recompression pulse fronts at the plate surface. The failure wave meets the unloading wave reflected from the glass free surface at the distance x and time moment t_x, as determined by

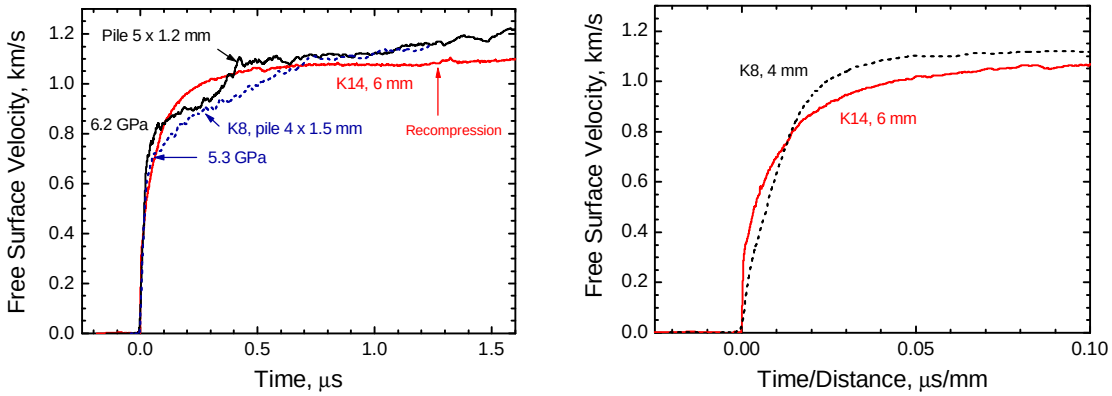

Fig. 3. Free surface velocity histories of single thick plate and assembled thin plates of K14 crown glass impacted by an aluminum flyer plate of 7 mm in thickness at 1.15 km/s velocity.

Fig. 4. Comparison of elastic compressive response of K8 and K14 crown glasses. The time is normalized by the sample plate thickness.

the following relationships

$$t_r = 2\frac{d-x}{c_l}, \text{ and } t_x = \frac{d}{c_l} + \frac{d-x}{c_l}$$

where δ is the glass plate thickness. The propagation velocity of the failure wave is given by

$$c_f = \frac{x}{t_x} = c_l \frac{2 - c_l t_r/\delta}{2 + c_l t_r/\delta}.$$

Using the sound speed value $c_l = 5.9$ km/s, $t_r = 1.25$ μs, $\delta = 6$ mm, we are estimating the failure wave speed in K14 crown glass $c_f = 1.41$ km/s that is slightly less than the failure wave speed in the soda lime glass.

3. Techniques of radial stressing

Controlled confinement pressure on the specimen is provided by installing a shrink-fit metal sleeve on the lateral surface of the cylindrical glass specimen. The samples are precisely cut disks of 22±0.002-mm diameter and 3.5-mm or 5 mm thickness. The shrink-fit steel rings of outer diameter 60 mm have been machined from normalized tool steel 45KhN2MFA having Yung modulus $E = 216$ GPa, Poisson's ratio $n = 0.28$, and the yield stress $s_{0.2} = 800$ MPa. The inside diameter of these compressive rings were cut to a diameter smaller than the diameter of the samples by misfit δ which was varied from 60 μm to 130 μm. Prior to the insertion of the sample discs, the rings were heated up to 600°C.

It is important to exclude any stress concentrations which may result in cracking the sample. Because of that, especial technology of assembling the pre-stressed samples was worked out. The technology and corresponding appliance are shown schematically in Fig. 5. Cold sample is glued onto plane end of the piston. The rest parts of appliance, including the guide bush and a

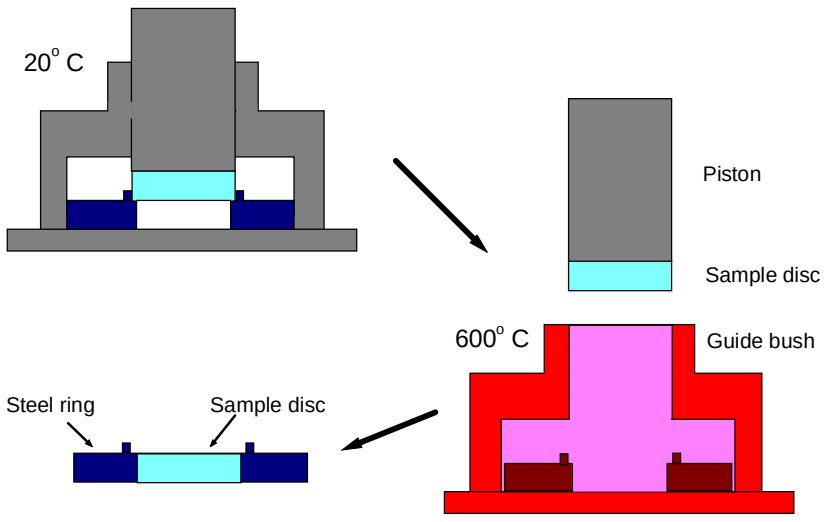

Fig. 5. The scheme of heavy-shrink fitting of the disk sample into the compressive ring.

holder are assembled with the compressive ring before their heating in a furnace. After that, cold piston with the sample disc is inserted into the guide brash and in this way the sample is inserted into the heated compressive ring. The piston/brash technology permits to minimize the tilt between the sample and the ring planes and to provide uniform and close contact of the sample and the ring surfaces. As a result of heating the sample and piston by other hot details of the appliance, the glue is burned out and the piston can be easy separated from the sample/ring assembly.

The confining stress p produced by the ring can be estimated by solving an axis-symmetric boundary value problem. For purely elastic deformation of the ring the solution is

$$p = \frac{d}{2R_c\left[\frac{1-n_c}{E_c} + \frac{R_s^2 + R_c^2 + n_s\left(R_s^2 - R_c^2\right)}{E_s\left(R_s^2 - R_c^2\right)}\right]},$$

where R_c is the sample radius, R_s is the ring outer radius, E_c, n_c, and E_s, n_s are the Young's moduli and Poisson's ratios of the sample and the ring materials, respectively. For the case of the elastic-perfect plastic behavior of the ring material the confining stress may be found from the expression

$$p = s_Y\left[\ln\left(R/R_c\right) + \frac{R_s^2 - R^2}{2R_s^2}\right],$$

where R is the radius of the boundary between elastically and plastically deformed regions of the ring and may be found from the equation

$$\left[\left(1-2n_s\right)\left(1+n_s\right)\frac{s_Y}{E_s} - \left(1+n_c^2\right)\frac{s_Y}{E_c}\right]\cdot\left[\ln\left(R_c/R\right) - \frac{R_s^2 - R^2}{2R_s^2}\right] + \left(1+n_s^2\right)\frac{s_Y}{E_s}\frac{R^2}{R_c^2} = \frac{d}{2R_c}.$$

In this way, the confining stress up to 215 MPa was reached in the glass samples without their fracture. At higher radial stresses (~300 MPa) the samples were partly fractured by plane cracks oriented approximately perpendicular to the sample axis.

4. Influence of pre-stressing on propagation of the failure waves in glasses

The scheme of experimental arrangement is shown in Fig. 6. The shock loading was realized by impact of aluminum flyer plate. The impact surface of the glass sample plate was grinded in order to create large amount of the crack nucleation sites. The glass sample was placed on the PMMA or Teflon base plate in which the stress pulse of approximately triangular profile and desirable peak stress was formed. Using the VISAR laser Doppler velocimeter [13], the histories of velocity of the interface between the sample and the water "window" or the free surface velocity were recorded. For these measurements, aluminum foil 8 μm in thickness was glued by epoxy upon the sample surface.

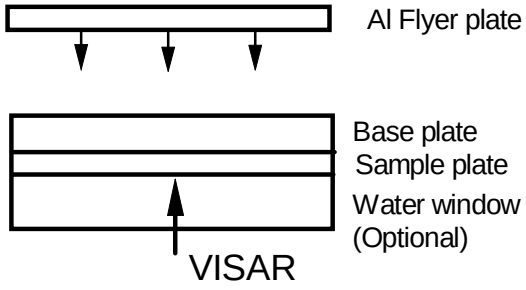

Fig. 6. The scheme of experimental arrangement for recording the failure wave phenomena at compression of the glass samples by a stress pulse of triangular profile.

In this arrangement, experiments with free and pre-stressed glass samples have been carried out. Figure 7 presets results of three shots with free K8 glass samples. The free surface velocity history demonstrates strong second compression wave which is a result of wave re-reflection inside the glass plate at the boundary between the intact and cracked glass. In the waveform measured at the glass/water interface this recompression wave has smaller magnitude but appears at approximately the same time moment. Comparison of the waveforms measured at different peak stresses distinctly demonstrates the stress dependence of the failure wave propagation. In Fig. 8 the free surface velocity history of K14 glass sample impacted in such way is compared with that from Fig. 3. One can see the time interval between the compression wave front and the recompression signal is essentially larger in the case of shorter load pulse.

The wave interactions for the impact conditions shown in Fig. 6 are illustrated in Figs 9 and 10. As a result of different dynamic impedances, impact of aluminum flyer plate upon the PMMA base plate produces in the latter shock pulse with step-wise unloading part [1]. Uniaxial compression above the failure threshold initiates the failure wave in glass plate but following unloading stops its propagation. After reflection of the compression wave from the sample free surface or the sample/window interface the reflected rarefaction wave interferes with incident

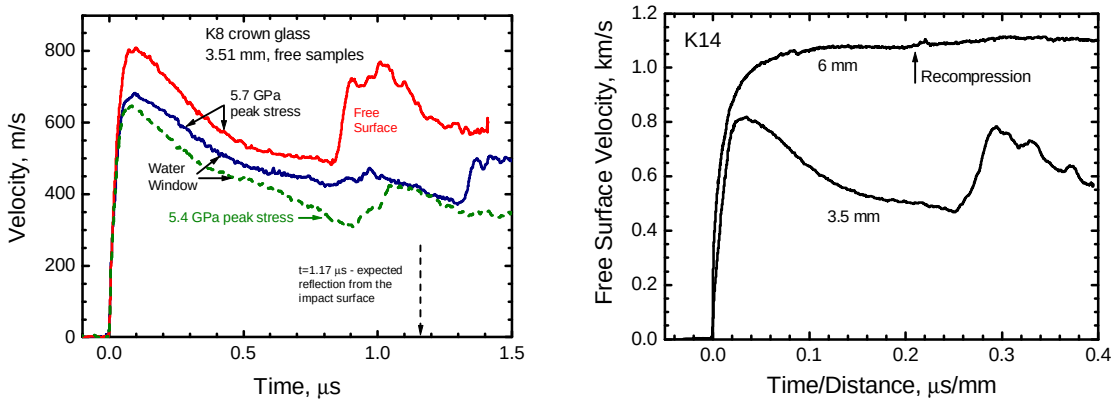

Fig. 7. Results of experiments with free samples of K8 crown glass impacted by aluminum flyer plates 2 mm in thickness through the PMMA base plates 7.9 mm in thickness (solid lines). Dashed line presents the waveform which has been obtained earlier using 1.42-mm-thick flyer plate and 6-mm-thick base plate. The wave reverberation time for undamaged glass t = 1.17 μs was estimated using the zero-stress value of longitudinal sound speed c_l = 6.0 km/s.

Fig. 8. Free surface velocity histories of K14 crown glass samples impacted by thick and thin flyer plates. The time is normalized by the sample plate thickness.

unloading wave and interacts with the material layer fractured by the failure wave. Dynamic impedance of fractured glass does not much differ from that of intact material. Due to this, interaction of reflected wave with fractured layer produces just weak recompression if the compressed state is kept. However the fracture results in loss of ability of resisting to tension. In the experiment with water window there is incomplete unlading at the sample/window interface. In this case the wave interaction at a boundary of cracked layer occurs in compressed state or at small tension and does not produce large reflection. In the experiments with free sample surface interaction of the incident and reflected unloading waves produces much larger tensile stresses at the tile of reflected wave (point K_f in Fig. 10). The tensile part of rarefaction wave interacts with the boundary of cracked layer in the same way as it does with free surface. As a result, much larger reflected compressive wave is produced.

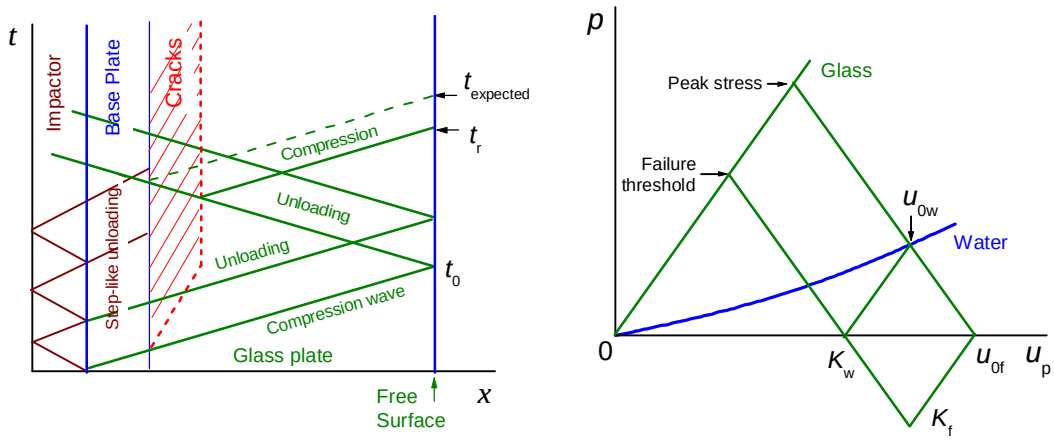

Fig. 9. The time-distance diagram of wave interactions for the impact conditions shown in Fig. 6.

Fig. 10. The pressure – particle velocity diagram of the wave interactions in glass sample tested with water window and without window.

Since the free surface velocity histories exhibit the recompression much more distinctly, following experiments were carried out in this mode, although quality of the VISAR signals was better in experiments with windows. In Fig. 11, the free surface velocity histories of K8 and K14 glasses are compared. Due to higher failure threshold of K14 glass the failure wave stops here earlier that explains larger time interval between the compression wave and reflected wave fronts.

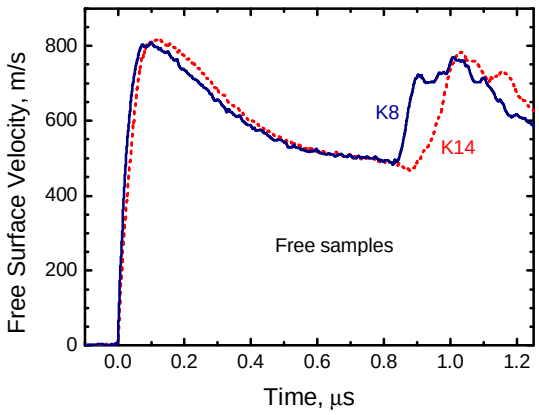

Fig. 11. Results of experiments with free samples of K8 and K14 crown glasses 3.5 mm in thickness under the same impact conditions.

Figures 12 and 13 present results of experiments with free and pre-stressed samples of K8 and K14 crown glasses. The measurements clearly demonstrate the influence of pre-stressing on the distance of the failure propagation which appears in decreased reverberation time. The effect is larger in the case of K14 glass which is characterized higher failure threshold. Also, pre-stressing resulted in small decrease of the peak stress in shock-compressed K8 glass.

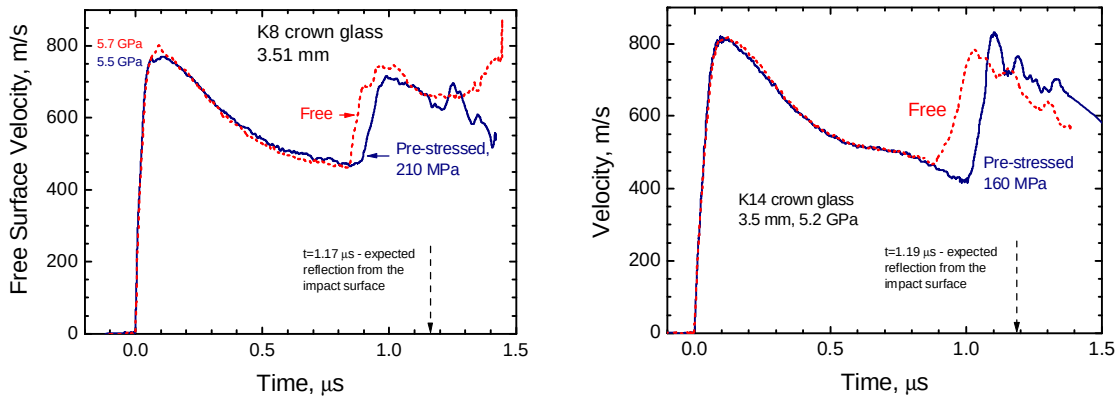

Fig. 12. Results of experiments with free and pre-stressed samples of K8 crown glass impacted by aluminum flyer plates 2 mm in thickness through the PMMA base plates 7.9 mm in thickness.

Fig. 13. Results of experiments with free and pre-stressed samples of K14 crown glass impacted by aluminum flyer plates 2 mm in thickness through the PMMA base plates 7.9 mm in thickness.

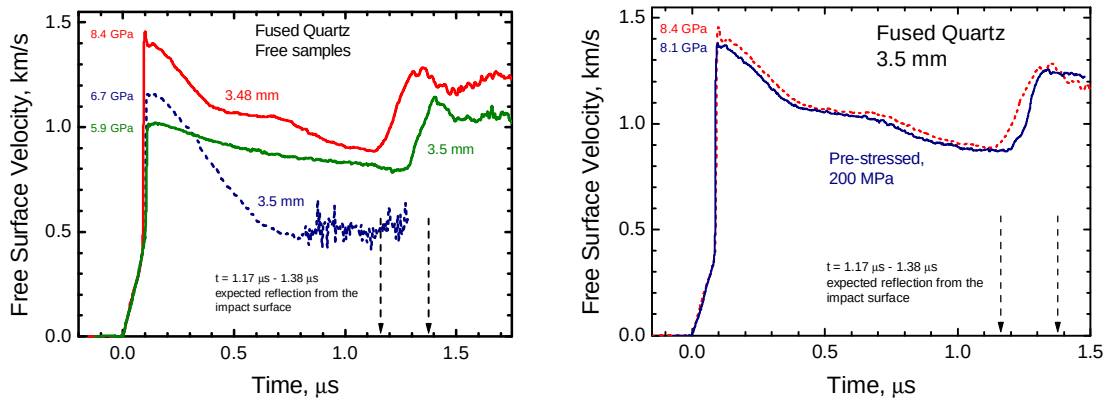

Fig. 14. Results of experiments with free samples of fused quartz. The wave reverberation times for undamaged material were estimated using the zero-stress value of longitudinal sound speed c_l = 5.95 km/s that gives t = 1.17 μs and minimum wave speed value 5.05 km/s in compressed fused quartz that gives t = 1.38 μs. The shock pulse of 5.9 GPa peak stress was generated by impact of aluminum flyer plate 4 mm in thickness through the PMMA base plate 18 mm in thickness at 1.5 km/s impact velocity. The shock pulse of 6.7 GPa peak stress was generated by impact of aluminum flyer plate 2 mm in thickness through the base plate assembled from 2 mm thick aluminum and 4.3 mm thick Teflon plates at 1.2 km/s impact velocity. The shock pulse of 8.4 GPa peak stress was generated by impact of aluminum flyer plate 2 mm in thickness through the PMMA base plate 8 mm in thickness at 1.9 km/s impact velocity.

Fig. 15. Results of experiments with free and pre-stressed samples of fused quartz impacted by aluminum flyer plate 2 mm in thickness through the PMMA base plate 8 mm in thickness at 1.9 km/s impact velocity.

Figure 14 presents results of experiments with free samples of fused quartz. Their goal was to find out optimal conditions for investigations of the pre-stress effects. In the figure, two estimations of wave reverberation time in undamaged plate are shown. It is known the fused quartz has anomalous compressibility at elastic uniaxial compression. This anomaly appears in the shape of elastic compression wave, the front of which propagates with the velocity c_l = 5.95 km/c whereas the end of its ramped part propagates with 5.05 km/s velocity. Correspondingly, the zero-stress value of longitudinal sound speed c_l = 5.95 km/s gives the reverberation time t = 1.17 μs, whereas minimum wave speed value 5.05 km/s gives t = 1.38 μs.

Earlier [11,12] the failure threshold at shock compression of fused quartz was estimated as 7 GPa to 7.7 GPa. Comparison of the waveforms at 8.4 GPa and 5.9 GPa peak stresses, that is slightly above and below the threshold, demonstrates different wave reverberation times. This time difference may be treated as an evidence of cracking near the impact surface. Comparison with estimated time of reverberation of elastic wave in undamaged plate shows that the cracking is bounded within thin layer near the impact surface.

Figure 15 presents results of experiments with free and pre-stressed samples of fused quartz. Again, the stress effect is demonstrated in delayed arrival of the recompression signal.

5. Influence of pre-stressing on propagation of shock compression waves in sapphire

Figure 16 presents results of three preliminary shots with free samples of sapphire. Experiments were done using different VISAR etalons in order to exclude uncertainty in amount of lost interference fringes and surely determine absolute values of the velocity. In all shots the quality of VISAR records was low. Obtained waveforms are strongly oscillated and are not reproducible in details. First short spike of 6-8 ns duration at the elastic precursor front is probably an effect of wave reverberation in the foil reflectors which were 20 μm in thickness in these shots. The high-frequency particle velocity jitter is evidence for heterogeneity of the inelastic deformation process. Another characteristic feature is the significant stress relaxation behind the elastic precursor front that is caused by intense multiplication of the deformation carriers [1].

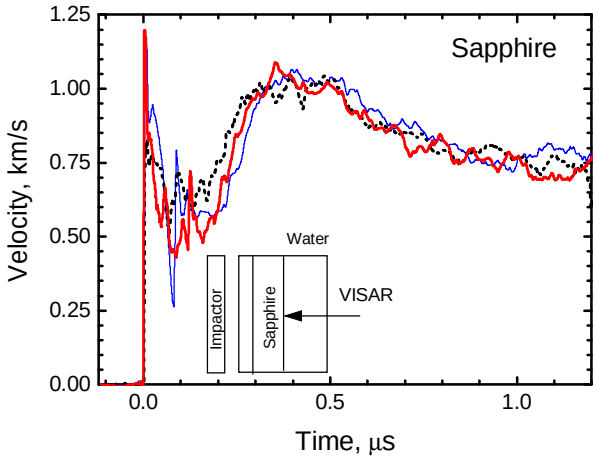

Fig. 16. Results of experiments with sapphire samples 5.02 mm in thickness impacted by aluminum flyer plates 2 mm in thickness at 1.9±0.05 km/s impact velocity. Experiments with water window.

Low quality and low repeatability of waveforms at the sapphire/window interface will not permit to reveal small pre-stress effects. The waveforms can be smoothed by averaging the velocity data over larger area. Since the VISAR beam must be focused into small spot, the averaging in further experiments was arranged by means of placing intermediate copper plate 2 mm in thickness on the sapphire sample surface. Dynamic impedance of copper does not much differ from that of sapphire. Chosen thickness of averaging copper plate was sufficient to provide about 1 μs wave reverberation time and corresponding record time without wave reflections.

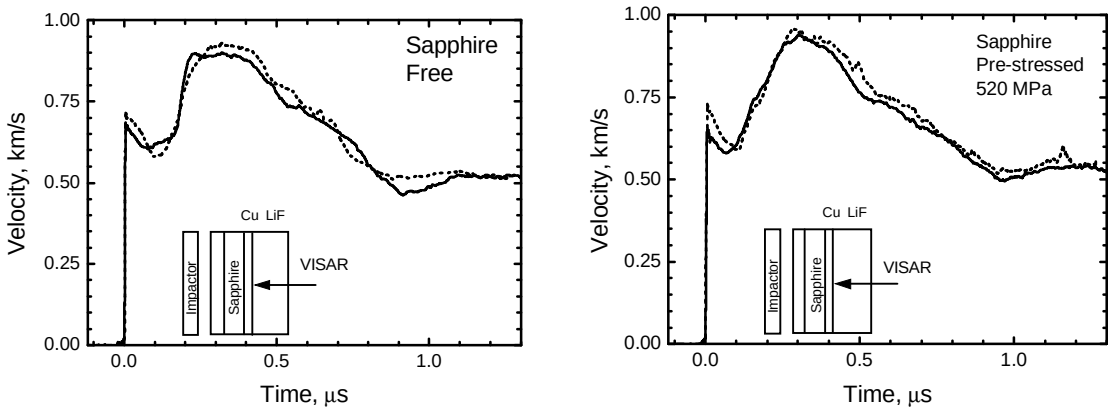

Fig. 17. Results of experiments with free sapphire samples 5.02 mm in thickness impacted by aluminum flyer plates 2 mm in thickness at 1.9 km/s impact velocity. Experiments with LiF window and averaging copper plate of 2-mm thickness.

Fig. 18. Results of experiments with pre-stressed sapphire samples 5.02 mm in thickness impacted by aluminum flyer plates 2 mm in thickness at 1.9 km/s impact velocity. Experiments with LiF window and averaging copper plate of 2-mm thickness.

Figures 17 and 18 present results of experiments with free and pre-stressed sapphire samples. Quality of the VISAR records in these shots was much better than that at measurements immediately at sapphire surface, measured waveforms are much less oscillated and are better reproduced. Nevertheless the scatter of parameters at the elastic precursor front is still too large from shot to shot and does not allow to evaluate dependence of the HEL value upon radial pre-stressing. On the other hand, there is obvious difference in the rise time of second (inelastic) compression wave.

Figure 19 compares waveforms in free and pre-stressed sapphire samples. Each wave profile has been obtained by averaging of two measured velocity histories presented in Figs. 17 and 18, correspondingly. From these data, maximum acceleration in second wave is 5×10^6 km/s^2 for free sample (the rise time from 0.1 to 0.9 of the magnitude is ~80 ns) and 2×10^6 km/s^2 for pre-stressed sample (140 ns of the rise time). Phenomenologically different rise times mean different viscosity of the matter.

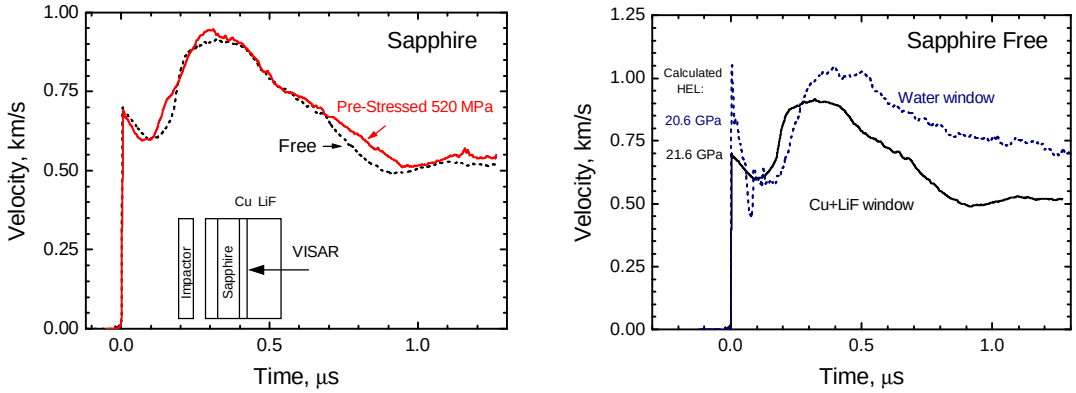

Fig. 19. Averaged velocity histories for free and pre-stresses sapphire samples. Original data are presented in Figures 17 and 18.

Fig. 20. Averaged velocity histories for free sapphire samples. Original data from experiments with LiF and water windows are presented in Figures 16 and 17.

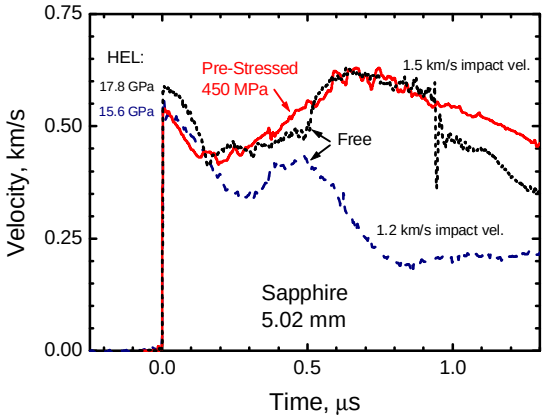

Fig. 21. Results of low-stress experiments with free and pre-stressed sapphire samples. Experiments with LiF window and averaging copper plate of 2-mm thickness. The shock load was created by impact of aluminum flyer plates 4 mm in thickness at the impact velocity 1.5±0.05 km/s and 2 mm in thickness at the impact velocity 1.2±0.05 km/s.

In order to estimate how much the waveforms are distorted by averaging copper plates, Figure 20 compares results of experiments with and without the plate. After the plate second wave indeed becomes steeper that means the difference in inelastic response of free and pre-stressed sapphire is not so large as it follows from Fig. 9, but nevertheless it undoubtedly exists. The HEL values evaluated from these data by the impedance mismatch method are around 21 GPa.

Figure 21 summarizes results of measurements at lower peak stresses. These data confirm influence of pre-stressing upon the rise time of second compression wave. The measurements confirm also earlier observed dependence of the HEL value on the peak stress [14]. In addition, intense stress relaxation after elastic shock compression has been recorded even at lowest peak stress 15.6 GPa where purely elastic response was expected. In this connection we would note

that Barker and Hollenbach [13] detected erratic optical behavior of sapphire at a shock stress of about 15 GPa. They interpreted this as an indication of the onset of plastic yielding.

6. Discussions and conclusions

Presented herein experimental data for sock-loaded free and pre-stressed glasses and sapphire crystals confirm our expectation of influence of transversal stress upon the response of homogeneous brittle materials to shock compression. For all pre-stressed glasses we observed earlier break of the failure wave propagation at unloading from shock-compressed state. Experiments with sapphire crystals experiments unambiguously demonstrate growth of viscosity of inelastic compression as a result of pre-stressing.

In order to estimate significance of observed effect of pre-stressing upon the failure wave phenomenon let us compare our results with theoretical prediction. Figure 22 illustrates influence of a lateral pre-stressing on the compressive failure threshold of brittle materials. Compressive fracture may be described by the Griffith's failure criterion

$$(s_1 - s_2)^2 = Y_{br}(s_1 + s_2)$$

which is based on the assumption that the failure starts when the highest local tensile stress at the longest crack of the most vulnerable orientation reaches a fixed critical value.

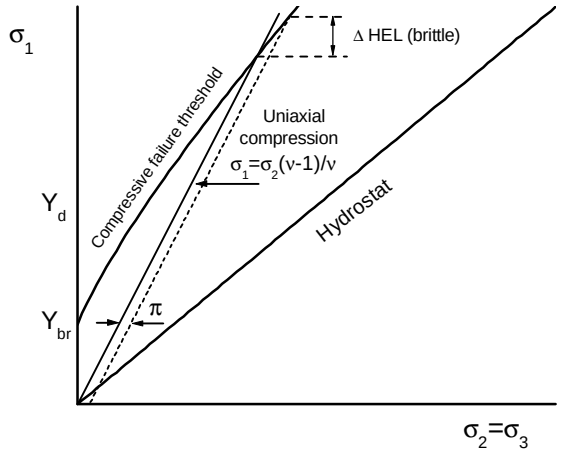

Fig. 22. Influence of a lateral pre-stressing on the compressive failure threshold.

Uniaxial elastic compression is described by the line $s_1 = s_2(1–n)/n$. Intersection of this line with the line imaging the criterion of compressive fracture in Fig. 22 determines the failure threshold at uniaxial shock compression. One can see that applying additional transversal confining stress π shifts the intersection point toward higher stresses. Sensitivity of the threshold value to small variations of transversal stress can be estimated as [4]:

$$\frac{ds_f}{dp} = \frac{(1-n)(3-2n)}{(1-2n)}$$

For glasses expected sensitivity is $ds_f/dp \approx 3.5$. On the other hand, using obtained experimental data, we may make quantitative estimation of the pre-stress effect Δs_f on the failure threshold s_f by means of comparing of time intervals Δt between incident and reflected compression wave fronts for free (Δt_f) and pre-stressed (Δt_s) glass samples using the relationship

$$\Delta s_f = r c_l \frac{\alpha_{fs}}{2} \frac{\Delta t_f - \Delta t_s}{2}$$

where α_{fs} is deceleration of the free surface in the unloading wave, r - density, c_l – longitudinal sound speed. For K8 crown glass at 215 MPa radial confinement stress $\Delta t_f - \Delta t_s = 0.05$ μs, $\alpha_{fs} = 0.75$ km/s/μs (Fig. 13) we obtain $\Delta s_f = 140$ MPa, $\Delta s_f/p = 0.65$. For K14 crown glass (Fig. 13) at 160 MPa radial confinement stress $\Delta t_f - \Delta t_s = 0.12$ μs, $\alpha_{fs} = 0.9$ km/s/μs we obtain $\Delta s_f = 400$ MPa, $\Delta s_f/p = 2.5$.

Thus, experiments with pre-stressed glasses demonstrate lower sensitivity of the fasilure threshold value to variations of transversal stress than it was expected in accordance with the Griffith's criterion whereas usually the dependencies $\sigma_1(\sigma_2)$ at the failure threshold are stronger than that predicted by this criterion [15]. Obviously, there are some physical phenomena which we did not account for our analysis. Probably, irreversible densification of glass under pressure contributes into the failure wave mechanisms.

Observed increase of the rise time in inelastic compression wave in sapphire may be treated in terms of post-failure deformation. Whereas mechanisms of plastic deformation are not very sensitive to pressure, the resistance to deformation of comminuted matter is determined by the inter-particle friction which strongly depends on the pressure. In this case observed effect may be considered as a confirmation of fracture of sapphire under shock compression.

Thus, performed experiments have reveals two new effects in behavior of brittle materials under shock compression. Further investigations are needed to make clear the nature and details of found phenomena.

References

1. G.I. Kanel, S.V. Razorenov, V.E. Fortov. Shock-Wave Phenomena and the Properties of Condensed Matter. Springer, New York, 2004, 320 pp.
2. W. Chen and G. Ravichandran. Static and dynamic compressive behavior of aluminum nitride under moderate confinement. *J. Am. Ceram. Soc*. **79**(3), 579-584 (1996).
3. W. Chen and G. Ravichandran. Failure mode transition in ceramics under dynamic multiaxial compression. *Internat. J. of Fracture,* **101**(1) 141-159 (2000).
4. E.B. Zaretsky and G.I. Kanel. Evidence of ductile response of alumina ceramic under shock wave compression. *Appl. Phys. Letters* **81**(7) 1192-1194 (2002)
5. E.B. Zaretsky, V.E. Paris, G.I. Kanel, and A.S. Savinykh. Evidence of Ductile (Alumina) and Brittle (Boron Carbide) Response of Ceramics under Shock Wave Loading. Ceramic Armor and Armor Systems. ed. E. Medvedovski, *Ceramic Transactions,* **151**, 105-115 (2003)
6. C. Han and C.T. Sun. A study of pre-stress effect on static and dynamic contact failure of brittle materials. *Int J Impact Eng*; 24(6–7), 597–611 (2000).
7. T.J. Holmquist, G.R. Johnson. Modeling prestressed ceramic and its effect on ballistic performance. *Int J Impact Eng* **31**(2), 113-127 (2005)
8. J.C.F. Millett and N.K. Bourne. Effect of internal strain on the propagation of failure in shock loaded soda-lime glass. *J. Appl. Phys.* **95**(9), 4681-4687 (2004).
9. G.I. Kanel, S.V. Razorenov, A. S. Savinykh, A. Rajendran, Zhen Chen. A study of the failure wave phenomenon in glasses compressed at different levels. J. Appl. Phys. **98**, 113523 (2005)
10. G.I. Kanel. Failure waves in shock-compressed glasses. In: Shock Compression of Condensed Matter – 2005, Eds.: M.D. Furnish et al., AIP Conference Proceedings **845**, New York, 2006, p. 870-875
11. G.I. Kanel, A.A. Bogatch, S.V. Razorenov, A.S. Savinykh. A systematic study of the failure wave phenomenon in brittle materials. *Report for ERO contract N62558-02-M-6020* (2003).
12. G. I. Kanel, A. A. Bogach, S. V. Razorenov, A. S. Savinykh, Z. Chen, and A. Rajendran. A Study of the Failure Wave Phenomenon in Brittle Materials. In: Shock Compression of Condensed Matter – 2003, Eds. M. D. Furnish et al., AIP CP **706**, pp. 739-742 (2004).
13. L.M. Barker and Hollenbach R.E. Shock-wave studies of PMMA, fused silica, and sapphire. *J. Appl. Phys.*, 41, 4208–4226 (1970).
14. R.A. Graham and W.P. Brooks. Shock-wave compression of sapphire from 15 to 420 kbar. The effects of large anisotropic compression. - *J. Phys. Chem. Solids*, **32**, 2311–2330 (1971).
15. McClintock, F.A. and Argon, A.S. *Mechanical behavior of materials.* Addison-Wesley Publ (1966).

REPORT DOCUMENTATION PAGE

Form Approved
OMB No. 074-0188

1. AGENCY USE ONLY.	2. REPORT DATE	3. REPORT TYPE AND DATES COVERED
	March 20, 2007	Final Report, March 1 2006 – March 1 2007

4. TITLE AND SUBTITLE

A STUDY OF PRE-STRESS EFFECT ON DYNAMIC FAILURE OF TRANSPARENT BRITTLE MATERIALS

5. FUNDING NUMBERS

Grant # **RUE2-1615-MO-06**

6. AUTHORS

G.I. Kanel, S.V. Razorenov, A.S. Savinykh, G.S. Bezruchko, G.V. Garkushin, G.E. Ivanchikhina

7. PERFORMING ORGANIZATION NAME(S) AND ADDRESS(ES)

INSTITUTE FOR HIGH ENERGY DENSITIES
RUSSIAN ACADEMY OF SCIENCES
IVTAN, IZHORSKAYA 13/19
MOSCOW 127412, RUSSIA

8. PERFORMING ORGANIZATION REPORT NUMBER

9. SPONSORING / MONITORING AGENCY NAME(S) AND ADDRESS(ES)

USAITC-A,
U.S. CIVILIAN RESEARCH AND DEVELOPMENT FOUNDATION
1530 Wilson Boulevard, Third Floor
Arlington, Virginia 22209

10. SPONSORING / MONITORING AGENCY REPORT NUMBER

11. SUPPLEMENTARY NOTES

12a. DISTRIBUTION / AVAILABILITY STATEMENT

12b. DISTRIBUTION CODE

13. ABSTRACT

The report presents results of studying the pre-stress effect on dynamic failure of K8 crown glass, K14 crown glass, fused quartz and sapphire crystals. A technology of radial pre-compression of glass samples has been worked out. Controlled confinement pressure on the specimen in a range of 150 MPa to 550 MPa was provided by installing a shrink-fit metal sleeve on the lateral surface of the glass specimen disk. Results of measurements of the particle velocity histories of sock-loaded free and pre-stressed glasses confirm our expectation of influence of transversal stress upon the failure wave propagation and the failure threshold: for all pre-stressed glasses we observed earlier break of the failure wave propagation at unloading from shock-compressed state. However, sensitivity of the failure threshold to the confinement stress value is not as high as it could be expected. Large heterogeneity of inelastic deformation and scatter in the Hugoniot elastic limit of sapphire have not allowed us to determine an influence of pre-stressing on the HEL value of this material. However, the experiments unambiguously demonstrate growth of viscosity of inelastic compression of the sapphire as a result of pre-stressing.

14. SUBJECT TERMS	15. NUMBER OF PAGES
Shock waves, failure waves, glasses, sapphire	19
	16. PRICE CODE

17. SECURITY CLASSIFICATION OF REPORT	18. SECURITY CLASSIFICATION OF THIS PAGE	19. SECURITY CLASSIFICATION OF ABSTRACT	20. LIMITATION OF ABSTRACT

NSN 7540-01-280-5500

Standard Form 298 (Rev. 2-89)
Prescribed by ANSI Std. Z39-18
298-102